Higher-order protection of quantum gates: Hamiltonian engineering coordinated with dynamical decoupling

P. Z. Zhao, ¹ Tianqi Chen, ^{1,2} Sirui Liu, ^{2,3,4} and Jiangbin Gong ^{1,2,4,*}

¹Center for Quantum Technologies, National University of Singapore, Singapore 117543, Singapore
 ²Department of Physics, National University of Singapore, Singapore 117551, Singapore
 ³Department of Chemistry, National University of Singapore, Singapore 117543, Singapore
 ⁴Joint School of National University of Singapore and Tianjin University,
 International Campus of Tianjin University, Binhai New City, Fuzhou 350207, China
 (Dated: September 23, 2024)

Dynamical decoupling represents an active approach towards the protection of quantum memories and quantum gates. Because dynamical decoupling operations can interfere with system's own time evolution, the protection of quantum gates is more challenging than that of quantum states. In this work, we put forward a simple but general approach towards the realization of higher-order protection of quantum gates and further execute the first cloud-based experimental demonstration of dynamical-decoupling-protected quantum gates at the first order and the second order. The central idea of our approach is to engineer (hence regain the control of) the gate Hamiltonian in coordination with higher-order dynamical decoupling sequences originally proposed for the protection of quantum memories. The physical demonstration on an IBM quantum processor indicates the effectiveness and potential of our approach on noisy intermediate scale quantum computers.

INTRODUCTION

A crucial challenge in implementing quantum computation is to overcome the decoherence induced by both internal and external environments of a quantum computer. Quantum error correction protocols make it possible to reliably storage and process quantum information over long time scales, conditional upon that the noise level in individual quantum gates is below a certain threshold [1, 2]. However, reaching the required low-noise threshold for fault-tolerant quantum computation is still challenging for physical implementations today. It is thus highly beneficial to execute active protection schemes for individual physical qubits to enhance quantum gate fidelity.

As an active approach, dynamical decoupling (DD) aims to average out the system-environmental interaction and hence protects either quantum memories or quantum gates [3, 4]. For quantum memories, periodic DD (PDD) [5] eliminates the effect of system-environment interaction to the first order (e.g., in the sense of a Magnus expansion), whereas concatenated DD (CDD) [6] and Uhrig DD (UDD) [7-10] can offer higher-order elimination of decoherence [11–14]. Experimental advances on DD-based quantum memory protection have been highly successful [15–20], with the recent benchmarking studies of DD carried out on actual noisy quantum computers [21, 22]. However, most of these experimental progresses on quantum memory protection have not been translated to the protection of quantum gates, because DD operations often interfere with quantum gate operations, e.g., DD pulses tend to freeze system's own time evolution.

One solution towards the DD protection of quantum gates started with choosing a dagger-closed DD group algebra, under which the system Hilbert space will include a subsystem where DD pulses applied to the system act like an identity operator on this subsystem [23, 24]. Then, this subsystem can be used to encode a qubit and the commutant of the group algebra can be used to perform computation under DD. However, the implementation of the coupling between such subsystemencoded qubits is rather complicated, making this route an experimental challenge. The second solution is to choose certain driving Hamiltonian commutable with DD operations [25– 27], the so-called "non-interference" condition. However, it is difficult to satisfy the non-interference condition when performing universal quantum gates on general single physical qubits. It is also highly nontrivial to construct the commutable driving Hamiltonian when combining DD with other noisemitigating strategies such as quantum error correction [28] and decoherence-free subspaces [29]. Therefore, this stimulating route needs extra physical-qubit resources to encode logical qubits, the implementation of which is often based on particular dynamical symmetries or specific qubit-qubit interactions to meet the non-interference requirement [30–32]. The third solution is based on the average Hamiltonian theory, where the gate operations are inserted between equidistant DD pulses such that $U = U_{N+1} \prod_{n=1}^{N} P_n U_n$. Here, P_n denotes the propagator of DD pulses and $U_n = \exp(-iH_{C_n}\tau_n)$ represents the time evolution between the DD pulses, induced by the gate Hamiltonian H_{C_n} . The explicit form of the driving Hamiltonian H_{C_n} , which yields the unitary operator U_n , is determined by the equation $\tilde{H}_{C_n} = T_n^{-1} H_{C_n} T_n$ in the so-called toggling frame of DD sequence, where $T_n = \prod_{k=1}^{n-1} P_k$ with $T_1 = T_{N+1} = I$. This approach typically extends the total gate time and can only realize first-order protection [33–35].

To fill in the gap between quantum memory protection and quantum gate protection, the dynamically corrected gate (DCG) was proposed as a sophiticated composite quantum gate constructed from primitive building blocks without encoding [42, 43]. DCG may offer higher-order protection with a concatenate design [44], but the total number of the required

^{*} phygj@nus.edu.sg

gate operations will be huge and thus there is essentially no experimental progress so far. By contrast, this work aims to show that higher-order protection of quantum gates can be directly achieved on general physical qubits, based on an experiment friendly Hamiltonian engineering approach plus well-known protocols designed for quantum memory protection. Indeed, the central idea of our higher-order protection approach lies in the engineering of the time dependence of system's driving Hamiltonian [5], in coordination with known higher-order DD sequences, such as CDD, UDD, and even nested UDD. As seen below, our engineering of system's driving Hamiltonian is to act against the unwanted impact of DD pulses on the system. This being done, only the systemenvironment interaction part is suppressed to higher orders and we recover our control over system's driving Hamiltonian. The DD protection of quantum memories and quantum gates can thus be unified and applied on an equal footing.

To date one-qubit gates can be executed at very high fidelities [36–38]. Our higher-order approach allows to execute one-qubit gates over a much longer duration. The extended execution time for one-qubit gates can be particularly crucial for hybrid quantum systems involving different types of qubits (e.g., the electron and nuclear spins of NV centers in diamond) where different qubits with markedly different operational time scales need to be synchronized [35, 39–41]. For two-qubit gates, our approach offers higher gate fidelity using single-qubit gates as the DD pulses. This indicates a new philosophy towards the design of basic building blocks for twoqubit gates: high-fidelity two-qubit gates may be composed by a series of available high-fidelity single-qubit gates together with engineered two-qubit gate Hamiltonians. In addition to numerical experiments to illustrate the performance of our higher-order protection schemes, we perform the first cloudbased experimental demonstration of DD-protected quantum gates at the first or the second order, verifying the effectiveness of our approach on an actual IBM quantum processor.

RESULTS

Approach. Consider a quantum system coupled to its environment with the total Hamiltonian $H(t) = H_{\rm S}(t) + H_{\rm E} + H_{\rm I}$. Here, $H_{\rm S}(t)$ is our system's driving Hamiltonian, $H_{\rm E}$ is the environment Hamiltonian and $H_{\rm I}$ is the system-environment interaction Hamiltonian. Using one-qubit system as an example, the general interaction between a qubit and its environment is in the form $H_{\rm I} = \sigma_x \otimes E_x + \sigma_y \otimes E_y + \sigma_z \otimes E_z$, where $E_{x(y,z)}$ represent the associated environment operators. To illustrate the underlying principle of our idea, we start with the protection of quantum gates under the PDD. For our purpose, we nest a periodic DD sequence $\{\sigma_0 \equiv I, \sigma_1 \equiv \sigma_x, \sigma_2 \equiv \sigma_y, \sigma_3 \equiv \sigma_z\}$ (I corresponding to no pulse applied) in between the time evolution governed by the driving Hamiltonian. The total evolution

operator is then given by

$$\mathcal{U} = \prod_{k=0}^{3} \sigma_{k} \left[\mathcal{T} e^{-i \int_{k_{\tau}}^{(k+1)\tau} H(t) dt} \right] \sigma_{k}$$

$$= \prod_{k=0}^{3} \mathcal{T} e^{-i \int_{k_{\tau}}^{(k+1)\tau} \sigma_{k} H_{S}(t) \sigma_{k} dt} e^{-i \left[\sum_{l=0}^{3} \sigma_{l} H_{I} \sigma_{l} + 4H_{E} \right] \tau} + O(\tau^{2}), \quad (1)$$

where the term with the smallest k is placed at the right most and \mathcal{T} denotes the time ordering. Note that $\sum_{l=0}^{3} \sigma_l H_I \sigma_l = 0$, so we have

$$\mathcal{U} = \prod_{k=0}^{3} \mathcal{T} e^{-i \int_{k\tau}^{(k+1)\tau} \sigma_k H_{S}(t) \sigma_k dt} \otimes e^{-i4H_{E}\tau} + O(\tau^2). \tag{2}$$

Clearly then, the first-order effect arising from $H_{\rm I}$ is eliminated. It is also seen that the time evolution of the quantum system is strongly influenced by the DD pulses. Indeed, during each time interval of duration τ , the effective Hamiltonian [the exponentials in Eq. (2)] is updated by the DD pulses.

Let us now unravel a key observation behind our Hamiltonian engineering approach. Denote the effective Hamiltonians altered by DD pulses associated with the time interval $[k\tau, (k+1)\tau]$ as $H_k(t) \equiv \sigma_k H_S(t)\sigma_k$. As an example, we take the driving Hamiltonian of the quantum system as $H_S(t)$ = $\Omega_x(t)\sigma_x + \Omega_y(t)\sigma_y$, where $\Omega_x(t)$ and $\Omega_y(t)$ are time-dependent parameters. One can then obtain $H_0(t) = \Omega_x(t)\sigma_x + \Omega_y(t)\sigma_y$, $H_1(t) = \Omega_x(t)\sigma_x - \Omega_y(t)\sigma_y$, $H_2(t) = -\Omega_x(t)\sigma_x + \Omega_y(t)\sigma_y$ and $H_3(t) = -\Omega_x(t)\sigma_x - \Omega_y(t)\sigma_y$, namely, the DD pulses affect the effective Hamiltonians associated with different time intervals through altering the signs of the parameters $\Omega_x(t)$ and $\Omega_{\rm v}(t)$. To fight against these changes to the system Hamiltonian imposed by the DD pulses, we adjust the parameters for different time intervals as $\Omega_{\rm r}(t) = \Omega(t)\cos\varphi$ and $\Omega_{v}(t) = \Omega(t) \sin \varphi$ for $t \in [0, \tau], \Omega_{x}(t) = \Omega(t) \cos \varphi$ and $\Omega_{v}(t) = -\Omega(t)\sin\varphi$ for $t \in (\tau, 2\tau], \Omega_{x}(t) = -\Omega(t)\cos\varphi$ and $\Omega_{v}(t) = \Omega(t) \sin \varphi$ for $t \in (2\tau, 3\tau]$, and $\Omega_{x}(t) = -\Omega(t) \cos \varphi$ and $\Omega_{v}(t) = -\Omega(t)\cos\varphi$ for $t \in (3\tau, 4\tau]$. Because $\Omega(t)$ is identified as the Rabi frequency of the qubit Hamiltonian and φ represents a phase of the driving field coupling the two levels of the qubit, the above adjusting can be implemented by only quenching the phase parameter of the driving field, reading φ for $t \in (0, \tau]$, $-\varphi$ for $t \in (\tau, 2\tau]$, $-\varphi + \pi$ for $t \in (2\tau, 3\tau]$ and $\varphi + \pi$ for $t \in (3\tau, 4\tau]$. With phase parameters quenched in this manner, one has $H_k(t) = \Omega(t)(\cos\varphi\sigma_x + \sin\varphi\sigma_y)$. That is, the effective Hamiltonians become the common Hamiltonian $\Omega(t)(\cos\varphi\sigma_x + \sin\varphi\sigma_y)$ over all time intervals. If we further require $\int_0^{4\tau} \Omega(t)dt = \theta/2$, Eq. (2) indicates

$$\mathcal{U} = e^{-i\theta(\cos\varphi\sigma_x + \sin\varphi\sigma_y)/2} \otimes e^{-i4H_E\tau} + O(\tau^2). \tag{3}$$

As such, to the first order of τ , the system-environment coupling is eliminated and yet we still implement a gate operation, namely, rotating the qubit along an axis in the xy plane by angle θ . Remarkably, this is achieved without requiring that $H_{\rm S}(t)$ commutes with the DD operations.

We are now ready to engineer the time dependence of the qubit Hamiltonian for higher-order protection of quantum gates. As an example, we consider the second-order protection by CDD. To that end, we use the time evolution protected by the DD operations $\{\sigma_0, \sigma_1, \sigma_2, \sigma_3\}$ as the basic building block and then nest it with a second layer of DD operations $\{\sigma_0, \sigma_1, \sigma_2, \sigma_3\}$. In doing so, we examine how the time dependence of $H_S(t)$ should be engineered. The evolution operator with two layers of DD operations is given by

$$\mathcal{U} = \prod_{m=0}^{3} \sigma_{m} \left[\prod_{k=0}^{3} \mathcal{T} e^{-i \int_{k\tau/4}^{(k+1)\tau/4} \sigma_{k} H_{S}(t) \sigma_{k} dt} \right] \sigma_{m} \otimes e^{-i4H_{E}\tau} + O(\tau^{3})$$

$$= \prod_{m=0}^{3} \prod_{k=0}^{3} \mathcal{T} e^{-i \int_{k\tau/4}^{(k+1)\tau/4} (\sigma_{m}\sigma_{k}) H_{S}(t) (\sigma_{k}\sigma_{m}) dt} \otimes e^{-i4H_{E}\tau} + O(\tau^{3}),$$
(4)

where all the terms in the product should be arranged from right to left with increasing k or m. We can analogously define the function appearing in the exponential as the effective Hamiltonian $H_{mk}(t) \equiv (\sigma_m \sigma_k) H_{\rm S}(t) (\sigma_k \sigma_m)$. Taking the driving Hamiltonian as $H_{\rm S}(t) = \Omega_x(t) \sigma_x + \Omega_y(t) \sigma_y$ again, we can easily obtain the explicit form of the effective Hamiltonian. Just like the previous example showcasing first-order protection, here we can also quench the phase φ without changing the Rabi frequency $\Omega(t)$ during time intervals as well as subintervals such that $H_{mk}(t) = \Omega(t)(\cos\varphi\sigma_x + \sin\varphi\sigma_y)$. With $\int_0^{4\tau} \Omega(t) dt = \theta/2$, we have

$$\mathcal{U} = e^{-i\theta(\cos\varphi\sigma_x + \sin\varphi\sigma_y)/2} \otimes e^{-i4H_E\tau} + O(\tau^3), \tag{5}$$

indicating that our one-qubit gate with second-order protection is achieved. It is straightforward to extend our approach to cases of higher-order protection of quantum gates by increasing the concatenation level of CDD.

Let us now turn to more efficient higher-order protection of quantum gates. According to the UDD theory proposed for quantum memory protection, the pure dephasing term $\sigma_z \otimes E_z$ can be filtered by applying nonequidistant decoupling operator σ_x . Likewise, the longitudinal relaxation term $\sigma_x \otimes E_x + \sigma_y \otimes E_y$ can be suppressed by applying σ_z operations at special UDD timings [7–10]. Building upon this, in order to average out general system-environmental interaction $H_I = \sigma_x \otimes E_x + \sigma_y \otimes E_y + \sigma_z \otimes E_z$, we apply n decoupling operations σ_x to the quantum system at times $t_j = 4\tau \sin^2[j\pi/(2n+2)]$, and during each time interval $[t_{j-1}, t_j]$, we further apply n decoupling operations σ_z at times $t_j^i = t_j \sin^2[k\pi/(2n+2)]$, where j, k = 1, ..., n and n is taken as an even number to facilitate our engineering approach. Such a nested UDD protocol yields the following time evolution operator:

$$\mathcal{U} = \mathcal{U}(4\tau, t_n) \prod_{j=1}^{n} \sigma_x \mathcal{U}(t_j, t_{j-1})$$

$$= \prod_{i=1}^{n+1} \sigma_x^{j-1} \mathcal{U}(t_j, t_{j-1}) \sigma_x^{j-1}, \qquad (6)$$

where $t_0 \equiv 0$, $t_{n+1} \equiv 4\tau$, all the terms in the product from right to left are arranged to have an increasing j, and $\mathcal{U}(t_j, t_{j-1})$, the unitary evolution operator associated with the interval $[t_{j-1}, t_j]$, is expressed by a product of subinterval evolution operators $\tilde{\mathcal{U}}(t_k^j, t_{k-1}^j)$ as

$$\mathcal{U}(t_j, t_{j-1}) = \tilde{\mathcal{U}}(t_j, t_n^j) \prod_{k=1}^n \sigma_z \tilde{\mathcal{U}}(t_k^j, t_{k-1}^j)$$

$$= \prod_{k=1}^{n+1} \sigma_z^{k-1} \tilde{\mathcal{U}}(t_k^j, t_{k-1}^j) \sigma_z^{k-1}$$
(7)

with $t_0^j \equiv t_{j-1}$ and $t_{n+1}^j \equiv t_j$, and all the terms in the product from right to left are arranged to have an increasing k. The UDD theory can guarantee that the effect of systemenvironment interaction is suppressed up to the nth order. That is,

$$\mathcal{U} = \prod_{j=1}^{n+1} \prod_{k=1}^{n+1} \mathcal{T}e^{-i\int_{j_{k-1}}^{j_{k}^{j}} \left(\sigma_{x}^{j-1}\sigma_{z}^{k-1}\right)H_{S}(t)\left(\sigma_{z}^{k-1}\sigma_{x}^{j-1}\right)dt} \otimes e^{-i4H_{E}\tau} + O(\tau^{n+1}). \tag{8}$$

To find out how to engineer the time dependence of the driving Hamiltonian $H_{\rm S}(t)$, we define effective Hamiltonians $H_k^j(t) \equiv (\sigma_x^{j-1}\sigma_z^{k-1})H_{\rm S}(t)(\sigma_z^{k-1}\sigma_x^{j-1})$, i.e., those terms appearing in the exponentials in the equation above. Using the same driving Hamiltonian introduced above, one obtains the effective Hamiltonian as $H_k^j(t) = (-1)^{k-1}\Omega_x(t)\sigma_x + (-1)^{k+j}\Omega_y(t)\sigma_y$, explicitly depicting the impact of our nested UDD operations on the system Hamiltonian. To combat against these unwanted changes to the system Hamiltonian, we can just adjust only the phase parameter of the qubit driving field, such that for $t \in [t_{k-1}^j, t_k^j]$, $\Omega_x(t) = (-1)^{k-1}\Omega(t)\cos\varphi$ and $\Omega_y(t) = (-1)^{k+j}\Omega(t)\sin\varphi$. The evident outcome of this phase quenching approach is that all the effective Hamiltonians will be the same, namely, $H_k^j(t) = \Omega(t)(\cos\varphi\sigma_x + \sin\varphi\sigma_y)$. Assuming $\int_0^{4\tau}\Omega(t)dt = \theta/2$, then one arrives at

$$\mathcal{U} = e^{-i\theta(\cos\varphi\sigma_x + \sin\varphi\sigma_y)/2} \otimes e^{-i4H_E\tau} + O(\tau^{n+1}), \tag{9}$$

which is a quantum gate protected by nested UDD to the *n*th order. To our knowledge, such a possibility of higher-order UDD protection of quantum gates is never shown before.

Our approach illustrated above can be extended to the engineering of various qubit-qubit interactions for higher-order protection of two-qubit operations. For instance, the higher-order protection of a controlled-phase gate can be implemented through engineering the following driving Hamiltonian

$$H_{\rm S} = J_1(t)\sigma_z^{(1)} + J_2(t)\sigma_z^{(2)} + J(t)\sigma_z \otimes \sigma_z, \eqno(10)$$

where J_1 and J_2 are the parameters of local operations respectively acting on the first and second qubits, and J is the coupling parameter between the two qubits. For the second-order protection with CDD, we analogously exploit the time

evolution protected by PDD operations $\{\sigma_0^{\otimes 2}, \sigma_1^{\otimes 2}, \sigma_2^{\otimes 2}, \sigma_3^{\otimes 2}\}$ as a basic building block and then nest it into a second layer of the same DD operations (so as to suppress all possible single-qubit errors during the two-qubit operation). As a result, the evolution operator over a period of 4τ yields the form in Eq. (4), with the effective Hamiltonians being expressed as $H_{mk}(t) \equiv (\sigma_m \sigma_k)^{\otimes 2} H_{\rm S}(t) (\sigma_k \sigma_m)^{\otimes 2}$. Using the effective Hamiltonians, it can be observed that the impact of DD pulses on the system Hamiltonian will not flip the sign of the qubit-qubit interaction term $J(t)\sigma_z\otimes\sigma_z$. In other words, only the sign of the single-qubit terms $J_1(t)\sigma_z^{(1)}$ and $J_2(t)\sigma_z^{(2)}$ may be changed. When this change does occur, we can just reverse the direction of the driving field to cancel the unwanted action of the CDD pulses. As an example where $|J_1(t)| = |J_2(t)| = J(t)$, our engineering protocol coordinated with the DD pulses will lead to $H_{mk} = -J(t)[\sigma_z^{(1)} + \sigma_z^{(2)} - \sigma_z \otimes \sigma_z]$. For $\int_0^{\bar{4}\tau} J(t)dt = \theta/2$, we obtain

$$\mathcal{U} = e^{-i\theta(-\sigma_z \otimes I - I \otimes \sigma_z + \sigma_z \sigma_z)/2} \otimes e^{-i4H_E \tau} + O(\tau^3). \tag{11}$$

Ignoring an unimportant global phase factor $\exp(i\theta/2)$, this gate under second-order protection yields $U = |00\rangle\langle00| + |01\rangle\langle01| + |10\rangle\langle10| + \exp(-i2\theta)|11\rangle\langle11|$, which is nothing but a protected controlled-phase gate.

Numerical experiments. Our higher-order protection promises to retain a high fidelity even for a slow one-qubit gate. For the two-qubit gate, the higher-order protection promises enhanced fidelity using single-qubit gates as DD operations. In the following, we demonstrate these through numerical experiments, with one particular focus on the impact of the finite duration of the DD operations on the performance of gate protection.

Let us consider the system-environment interaction physically originated from an isotropic Heisenberg coupling $\sigma_{r}^{s}\sigma_{r}^{b}$ + $\sigma_{y}^{s}\sigma_{y}^{b} + \sigma_{z}^{s}\sigma_{z}^{b}$ and an antisymmetric Dzyaloshinskii-Moriya coupling $\sigma_x^s \sigma_y^b - \sigma_y^s \sigma_x^b$ with a common coupling strength parameter ϵ for convenience [45, 46]. Here, the first spin represents the qubit of our system and the second spin represents the bath. We also assume that the bath spin is subject to a field Hamiltonian $\sigma_z + \sigma_x$ with the same strength ϵ for simplicity. Though simple, such a model construction captures the essence that the qubit system is subject to both dephasing and population relaxation and hence suffices to illustrate how our engineering approach leads to some higher-order protection. The spin-bath Hamiltonian adoped above may also model some residue interaction between a qubit system under gate operation and its surrounding qubits. The performance of our higher-order protection is characterized by the fidelity $F = \langle \phi | \rho | \phi \rangle$, where $| \phi \rangle$ is a target output state and ρ is a real output state.

For one-qubit gates, we set the initial state as $(|0\rangle + |1\rangle)/\sqrt{2}$, the ideal gate as $U = (\sigma_x + \sigma_y)/\sqrt{2}$ [the corresponding gate parameters are $\theta = \pi$ and $\varphi = \pi/4$, see Eq. (3)], and the system-bath coupling strength as $\epsilon = 2\pi \times 1$ MHz. Unless specified otherwise, the strength of our square-shaped DD pulse is

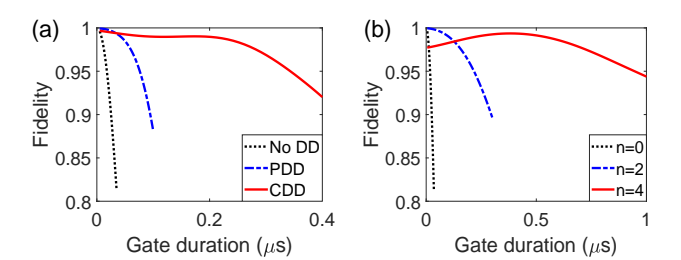


FIG. 1. The fidelity of a one-qubit gate changes with increasing the gate duration. (a) The fidelities under PDD with the first-order protection (blue) and CDD with the second-order protection (red), and without DD protection (black). (b) The fidelities under nested UDD protection with the orders n = 2 (blue) and 4 (red), and without DD protection (black).

chosen to be $2\pi \times 100$ MHz. This means that we utilize the finite-time gate operations rather than the ideal instantaneouspulse operations as our actual DD pulses. The DD protection of quantum gates is then performed by nesting the finite-time DD operations between the piecewise engineered time evolution according to the outlined approach. To illustrate how our higher-order protection can achieve a high fidelity of onequbit gates over a long time duration, we tune the gate duration 4τ over a wide range. In Fig. 1(a) we present the fidelity F vs the gate duration under the PDD and CDD with first-order and second-order protection, represented by the blue and red lines. As a comparison, we also plot the gate fidelity without any DD protection, as shown by the black line in the same figure. The results in Fig. 1(a) show that, while the first-order protection can already tolerate a longer gate duration than that of the bare gate, the second-order scheme offers a much better performance. For example, the first-order and second-order schemes yield gate fidelity > 95% for gate duration 0.075 μ s and $0.34 \mu s$, respectively, both being much longer than what the bare gate can last (0.018 μ s) at the same fidelity level. These results are encouraging because the applied DD pulses here have a finite width.

Next we investigate the performance of nested UDD in protecting one-qubit gate using our protocol outlined above. Figure 1(b) presents the gate fidelity with an increasing gate duration for second-order and fourth-order UDD, as shown by the blue and red lines, respectively (the gate fidelity without DD is represented by the black line). There it is seen that the second-order and fourth-order UDD protection retains the gate fidelity > 95\% for gate duration 0.21 μ s and 0.94 μ s, respectively, about 12 and 52 times longer than the duration $0.018 \,\mu s$ of a bare gate at the same fidelity level. It is interesting to note that such a great enhancement of gate duration at a high fidelity level using higher-order UDD protection is never shown before, even at the level of numerical experiments. Of course, the numerical findings here do not represent at all what one can achieve on an actual quantum computing platform, but still indicate that our higher-order protection approach of gate operations is indeed promising.

Finally, we turn to a two-qubit gate case. The ideal gate un-

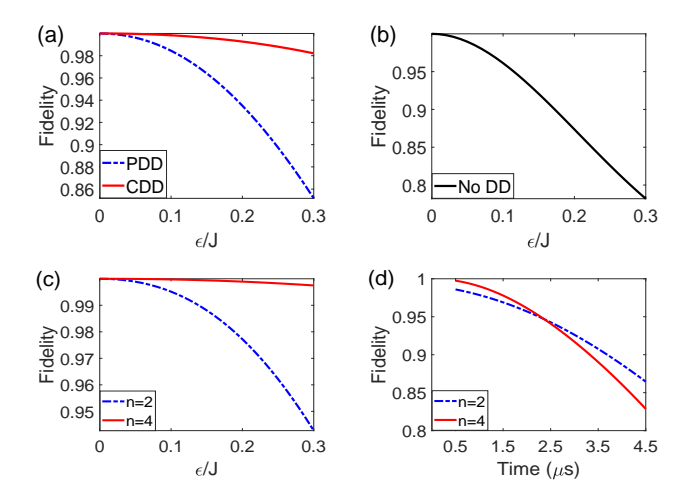


FIG. 2. The fidelity of a two-qubit gate using single-qubit operations as DD pulses. (a) The gate fidelity of PDD with the first-order protection (blue) and CDD with the second-order protection (red) vs the system-environment coupling strength over $\epsilon \in [0,0.3J]$. (b) The gate fidelity without protection for $\epsilon \in [0,0.3J]$. In both cases the duration of one single DD pulse is chosen to be 2.5 ns. (c) The gate fidelity under nested UDD protection with the orders of n=2 (blue) and 4 (red) for $\epsilon \in [0,0.3J]$, where the duration of one DD pulse is chosen as 0.5 ns for n=4 and 2.5 ns for n=2. (d) The gate fidelity vs the time duration of one DD pulse, namely, $\tau_{\rm DD} \in [0.5 \text{ ns}, 4.5 \text{ ns}]$ for n=2 (blue) and n=4 (red) with $\epsilon=0.3J$.

der consideration is $U = |00\rangle\langle 00| + |01\rangle\langle 01| + |10\rangle\langle 10| - |11\rangle\langle 11|$, the coupling parameter between two qubits is $J = 2\pi \times 5 \text{MHz}$ [see Eq. (10)], and the initial state is $(|00\rangle + |11\rangle)/\sqrt{2}$. In Fig. 2(a), we present the fidelity F vs the system-environment coupling strength over $\epsilon \in [0, 0.3J]$ under PDD (first-order) and CDD (second-order), represented by the blue and red lines. The gate fidelity without any DD protection is also plotted in Fig. 2(b) as a comparison. Since our numerical experiments only serve as a proof-of-principle verification, the two qubits are assumed to interact with a third qubit as the common bath, under the same qubit-bath interaction as in the above single-qubit case. The results here show that both firstorder and second-order protocols yield gate fidelities much better than that of the bare gate. Notably, for the case $\epsilon = 0.3J$, i.e., the system-environment coupling strength is 0.3 times of the gate Hamiltonian strength such that the fidelity of the bare gate is as low as 78.19%, the first-order protection of PDD can improve the fidelity to 85.17% while the second-order protection of CDD can boost the fidelity back to 98.21%.

Our numerical experiments can also illustrate the performance of our approach when using nested UDD to protect the two-qubit gate to the nth order. Figure 2(c) presents the corresponding gate fidelity with n=2 and 4 over a wide range $\epsilon \in [0,0.3J]$. The gate fidelity is seen to be greatly enhanced when increasing the order of protection. In the case of fourth-order protection, we need 24 non-instantaneous DD operations to both qubits and hence the duration of each individual DD operation will be more consequential. Results in Fig. 2(c) are obtained with the duration of DD operation shortened by a

factor of 5 for the fourth-order case. The resultant gate fidelity with the second- and fourth-order protection can be as high as 94.27% and 99.75%, respectively, even for a relatively large system-environment coupling strength $\epsilon = 0.3J$. To investigate the influence of DD duration on our higher-order protection, we further plot the gate fidelity F vs the duration of one single DD operation, namely, $\tau_{DD} \in [0.5 \text{ ns}, 4.5 \text{ ns}]$. The results are shown in Fig. 2(d), with the system-environment coupling strength $\epsilon = 0.3J$. One sees that the fidelity of fourth-order protection can reach 99% whereas the fidelity of second-order protection does not. Furthermore, the fidelities of the fourth-order and second-order protection intersect at $\tau_{DD} = 2.3$ ns, indicating that in real life applications with finite-time DD pulses that are not sufficiently short, the second-order nested UDD can be better than the fourth-order version because the latter also induce extra decoherence due to the use of a large number of finite-duration DD pulses.

Physical demonstration on an IBM quantum computer.

Having shown the feasibility of our higher-order protection of quantum gates through numerical experiments above, we shall now examine the actual performance of our approach on an IBM quantum computer. However, because our access to IBM hardware does not allow us to insert single-qubit gates within one two-qubit gate, we consider higher-order protection of the combination of a series of CNOT gates instead. To that end, we use the original Qiskit API [47] to realize the first- and second-order protection of CNOT gate series under PDD and CDD. It is worth emphasizing that this physical realization is the first cloud-based experimental demonstration of the DD protection of quantum gates on a quantum network.

For the first-order protection, we concatenate four blocks of quantum gates with the number of gates in each block being $m \in \{1, 2, 3, 4, 5\}$. Figure 3 shows two examples with m = 1and m = 3. We then insert the PDD sequence equidistantly between two neighboring blocks to implement the first-order protection. The PDD protocol elaborated in Eq. (1) requires us to sequentially insert σ_x (denoted by X) and σ_z (denoted by Z) single-qubit gates as the DD operations, also shown in Fig. 3. Most importantly, according to our Hamiltonian engineering strategy elaborated above, we can now coordinate the gate Hamiltonian to be applied in accord with the DD operations to be applied. That is, to counteract the interference of the inserted DD operations on the time evolution, we apply pre-engineered two-qubit gates instead of the targeted CNOT gate. Specifically, if within each block there is one CNOT gate, the four two-qubit gates to be applied to the four blocks are given by

$$U_{1} = |0\rangle\langle 0| \otimes I + |1\rangle\langle 1| \otimes \sigma_{x},$$

$$U_{2} = |1\rangle\langle 1| \otimes I + |0\rangle\langle 0| \otimes \sigma_{x},$$

$$U_{3} = |1\rangle\langle 1| \otimes I - |0\rangle\langle 0| \otimes \sigma_{x},$$

$$U_{4} = |0\rangle\langle 0| \otimes I - |1\rangle\langle 1| \otimes \sigma_{x}.$$
(12)

It is straightforward to verify that these deformed two-qubit gates will be transformed to the expected CNOT gate once

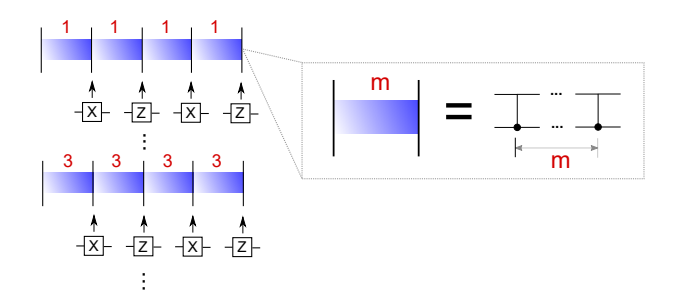


FIG. 3. The schematic for implementing the first-order protection of CNOT operations on an IBM quantum processor. Four blocks of quantum gates are concatenated with each block containing m gates. One-qubit gates are inserted according the PDD protocol between neighboring blocks to realize the first-order protection.

accounting for the interference of the PDD protocol. Interestingly, due to the explicit construction of the DD operation here, if within each block there is an even number of CNOT gates, then there is no need for such engineering because the overall action of these CNOT gates (which is identity) is not affected by the DD pulses. This being the case, if within each block there is an odd number of CNOT gates, we only need to engineer the first (or last) two-qubit gates in the jth block to be U_i defined in Eq. (12). With these arrangements, we examine the gate fidelity decay as a function of the duration to execute all the CNOT gates. For that purpose, we let τ denote the duration to execute 4 CNOT gates, with one block accommodating one CNOT gate. The raw counts are obtained from the sampling of quantum circuits execution on the IBM quantum processor. The results are shown in Fig. 4, with the initial state taken as $|00\rangle$ and each circuit executed for 10000 times. From the results, we can see that the first-order protection of the CNOT gates clearly offers an improvement of gate fidelity as compared with the unprotected case. This improvement becomes more obvious as the total number of executed CNOT gates increases.

Let us now turn to the physical demonstration of the second-order protection of CNOT gate series based on Hamiltonian engineering coordinated with the CDD protocol. Here we still concatenate four blocks of quantum gates, but in each block we stack two-qubit gates in the number of $m \in$ {4, 8, 12, 16}, as is shown in Fig. 5(a). Furthermore, we divide each block into four subblocks and hence there are sixteen subblocks in total. Accordingly, if m = 4, then each subblock accommodates only one two-qubit gate; whereas for m = 8, each subblock accommodates two two-qubit gates. We then insert the CDD sequence between the blocks and between the subblocks to implement the second-order protection. The actual one-qubit gates applied as DD operations at two different layers are indicated in Fig. 5(a). To counteract the interference of the CDD sequence on the targeted time evolution, we can now apply engineered gates coordinated with CDD, analogous to the above first-order case. In particular, for m = 4, the first four two-qubit gates in the first block are precisely

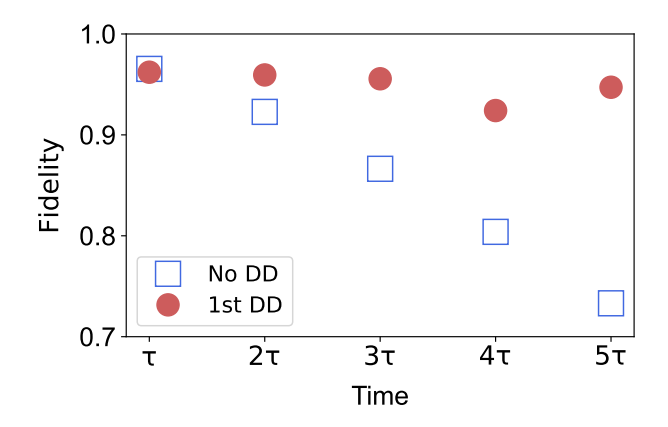


FIG. 4. The overall gate fidelity of combined CNOT gates under the first-order protection with PDD and Hamiltonian engineering, obtained from the IBM quantum processor. Here, the time unit $\tau = 2.64 \times 10^2$ ns represents the duration to execute totally 4 CNOT gates (one in each block). Fildelity in the case of 5τ is for a total of 20 combined CNOT gates. The results are obtained from ibm_kyoto hardware, and the total shots for each data is 10000.

the above-defined U_1 , U_2 , U_3 and U_4 in Eq. (12), followed by other 12 two-qubit gates chosen from U_1 , U_2 , U_3 and U_4 . The explicit sequence of all the 16 two-qubit gates is depicted in Fig. 5(b) using different colors. It is the overall action of these two-qubit gates plus the DD operations that may protect the CNOT gate series to the second order. The same sequence of two-qubit gates will be applied if $m = 4 \times (2r - 1)$, where r is a positive integer. If $m = 4 \times 2r$, i.e., each subblock contains an even number of CNOT gates, then their overall action within each subblock commutes with the DD operations, and hence there is no need to deform the CNOT gates, as also indicated in Fig. 5(b). To demonstrate that our Hamiltonian engineering approach of higher-order protection can operate in an integrated quantum circuit, we also deliberately introduce the crosstalk between the data qubits and some surrounding qubits. This is done by applying a controlled-Z gate to the data and surrounding qubits after every four CNOT gates, shown in Fig. 5(c). Figure 6 presents the overall fidelity of the combined CNOT gates under second-order protection vs the total time duration to execute the CNOT gates. For comparison, we also present the corresponding results obtained under the first-order protection and without any protection in the same figure. It is seen that the second-order protection clearly offers an enhanced fidelity compared with what can be achieved with bare CNOT gates. Furthermore, the fidelity with secondorder protection is slightly lower than that with first-order protection in the case of 16 CNOT gates. However, as the total number of CNOT gates increases, the case with second-order protection wins over the case with first-order protection. To our knowledge, our results here constitute the first-ever physical realization and demonstration of a higher-order protection of two-qubit gates.

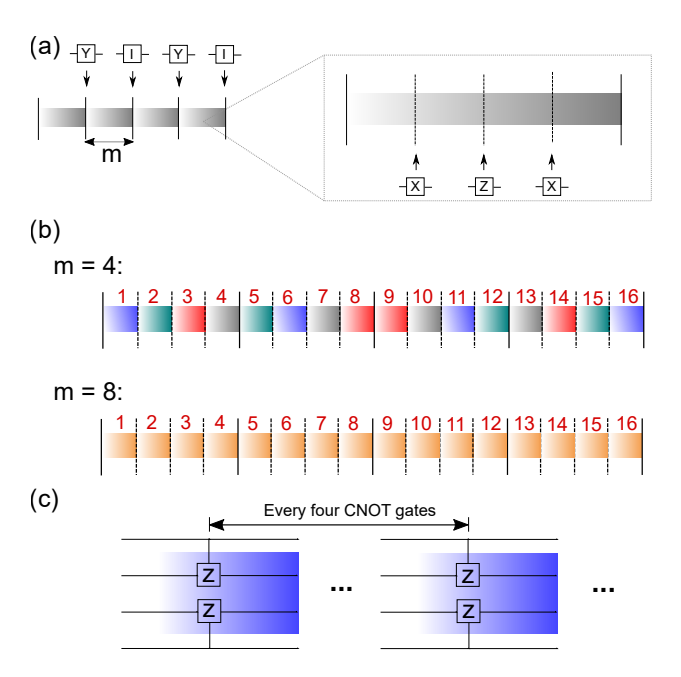


FIG. 5. The setup for implementing the second-order protection of CNOT gates on the IBM quantum processor, based on Hamiltonian engineering coordinated with CDD. (a) Four blocks of quantum gates are concatenated to form a noisy time evolution and each block is further divided into four subblocks with each subblock containing several two-qubit gates. The CDD sequence is then inserted to implement the second-order protection. (b) The engineered quantum gates when m=4 and 8. For m=4, the first four engineered gates U_1 , U_2 , U_3 and U_4 are represented by the first four colors, and the other 12 engineered gates chosen from U_1 , U_2 , U_3 and U_4 are depicted using different colors. For m=8, each color represents a CNOT gate. (c) Crosstalk between the data qubits and surrounding qubits is introduced by adding two surrounding qubits to the two-qubit quantum circuit along with a controlled-Z gate between the data qubit and surrounding qubit after every four CNOT gates.

DISCUSSIONS

The mitigation of noise and decoherence effects on the performance of quantum gates is a challenging optimization problem. This line of research, even at the one-qubit level [48–50], continues to advance quantum computing and quantum simulation technologies [51–59]. Machine learning techniques will play more important roles to realize robust quantum computing with optimized performance [60–62]. To guide future machine learning based optimization, some general principle towards higher-order protection of quantum gates would be extremely valuable in finding the optimal design of quantum gate Hamiltonians. In this work, we have shown that highly efficient schemes such as CDD and UDD for quantum memory protection can be used for the protection of quantum gates at different orders, provided that there is coordination between the DD operations and the time dependence of the gate Hamiltonians. To place a two-qubit gate under high-order protection, the basic building block may necessarily involve a number of high-fidelity single-qubit gates

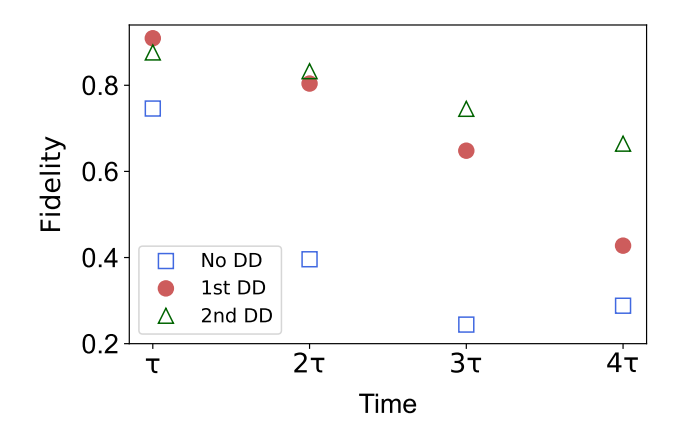


FIG. 6. The overall gate fidelity of combined CNOT gates under second-order protection on the IBM quantum processor, as compared with the corresponding results under first-order protection and no protection. Here, $\tau = 1.06 \times 10^3$ ns represents the duration to execute 16 CNOT gates (one CNOT gate in each subblock). Fildelity in the case of 4τ is for a total of 64 combined CNOT gates (four CNOT gates in each subblock). Note that the results for the first-order DD protection presented here are not achieved at the same time as those presented in Fig. 4, though obtained from the same ibm_kyoto hardware. The total shots for each data is 10000.

and the time dependence of the applied two-qubit gate Hamiltonian should be engineered accordingly.

This work has thus offered a promising starting solution towards optimized designs of robust quantum gates. Throughout, we only assume that the environment noise spectrum has a hard cutoff so that the higher-order schemes for quantum memory protection can work well (DD against an environment with a soft noise spectrum cutoff remains a challenge [63]). If there is more specific spectral information about the environment noises, then the time intervals between DD pulses can be further optimized according to the noise spectrum [64] and as a result, quantum gate protection using our concept can directly benefit from such optimization that can further drastically improve the performance of decoherence suppression. Our Hamiltonian engineering approach in coordination with DD hence makes the measurement of environment spectrum much more relevant than before to the realization of high-fidelity quantum gates.

Through numerical experiments using square-shaped pulses and physical demonstration on an IBM quantum processor, we have demonstrated that our approach is effective with noninstantaneous DD operations and hence experimentally feasible on noisy intermediate scale quantum computers. If pulse shaping is further introduced to the DD pulses and the driving Hamiltonians, then we foresee that higher-order protection scheme proposed in this work may further improve its performance. The long-term hope is that quantum gates protected under higher-order protection protocols can eventually provide a versatile toolbox to noisy intermediate scale quantum computers in the actual mitigation of decoherence, where a large number of gate operations will be applied in an inte-

grated and complex quantum circuit.

DATA AVAILABILITY

The datasets generated and analysed during the current study are available from the corresponding author on reasonable request.

ACKNOWLEDGMENTS

J. G. is grateful to Lorenza Viola for technical discussions and for her highly constructive comments on the first version of our manuscript. T. C. acknowledges Vinay Tripathi and Dario Poletti for fruitful discussions. We acknowledge the use of IBM Quantum services for this work via Singapore Quantum Engineering Programme (QEP). The views expressed are those of the authors, and do not reflect the official policy or position of IBM or the IBM Quantum team. This work was supported by the National Research Foundation, Singapore and A*STAR under its CQT Bridging Grant.

AUTHOR CONTRIBUTIONS

P. Z. Z. and J. G. conceived the basic idea of the project. P. Z. Z and S. L. conducted the computational demonstration. T. C. conducted the physical demonstration on IBM quantum processor. P. Z. Z. and J. G. wrote the paper. J. G. supervised the whole project.

COMPETING INTERESTS

The authors declare no competing interests.

- [1] Knill, E., Laflamme, R. & Zurek, W. H. Resilient quantum computation. *Science* **279**, 342 (1998).
- [2] Preskill, J. Reliable quantum computers. Proc. R. Soc. A 454, 385 (1998).
- [3] Viola, L., Knill, E. & Lloyd, S. Dynamical decoupling of open quantum systems. *Phys. Rev. Lett.* 82, 2417 (1999).
- [4] Viola, L., Lloyd, S. & Knill, E. Universal control of decoupled quantum systems. *Phys. Rev. Lett.* **83**, 4888 (1999).
- [5] Viola, L. & Knill, E. Robust dynamical decoupling of quantum systems with bounded controls. *Phys. Rev. Lett.* 90, 037901 (2003).
- [6] Khodjasteh, K. & Lidar, D. A. Fault-tolerant quantum dynamical decoupling. *Phys. Rev. Lett.* 95, 180501 (2005).
- [7] Uhrig, G. S. Keeping a quantum bit qlive by optimized π -pulse sequences. *Phys. Rev. Lett.* **98**, 100504 (2007).
- [8] W. Yang and R. B. Liu, Phys. Rev. Lett. 101, 180403 (2008).
- [9] West, J. R., Fong, B. H. & Lidar, D. A. Near-Optimal dynamical decoupling of a qubit. *Phys. Rev. Lett.* 104, 130501 (2010).

- [10] Wang, Z. Y. & Liu, R. B. Protection of quantum systems by nested dynamical decoupling. *Phys. Rev. A* 83, 022306 (2011).
- [11] Mukhtar, M., Saw, T. B., Soh, W. T. & Gong, J. Universal dynamical decoupling: Two-qubit states and beyond. *Phys. Rev. A* 81, 012331 (2010).
- [12] Mukhtar, M., Soh, W. T., Saw, T. B. & Gong, J. Protecting unknown two-qubit entangled states by nesting Uhrig's dynamical decoupling sequences. *Phys. Rev. A* 82, 052338 (2010).
- [13] Chen, K. & Liu, R. B. Dynamical decoupling for a qubit in telegraphlike noises. *Phys. Rev. A* **82**, 052324 (2010).
- [14] Wang, Z. Y. & Liu, R. B. Extending quantum control of time-independent systems to time-dependent systems. *Phys. Rev. A* 83, 062313 (2011).
- [15] Biercuk, M. J. et al. Optimized dynamical decoupling in a model quantum memory. *Nature* 458, 996 (2009).
- [16] Du, J. F. et al. Preserving electron spin coherence in solids by optimal dynamical decoupling. *Nature* 461, 1265 (2009).
- [17] Ryan, C. A., Hodges, J. S. & Cory, D. G. Robust decoupling techniques to extend quantum coherence in diamond. *Phys. Rev. Lett.* 105, 200402 (2010).
- [18] deLange, G., Wang, Z. H., Risté, D., Dobrovitski, V. V. & Hanson, R. Universal dynamical decoupling of a single solid-state spin from a spin bath. *Science* 330, 60 (2010).
- [19] Wang, Y. et al. Preservation of bipartite pseudoentanglement in solids using dynamical decoupling. *Phys. Rev. Lett.* 106, 040501 (2011).
- [20] Álvarez, G. A., Souza, A. M. & Suter, D. Iterative rotation scheme for robust dynamical decoupling. *Phys. Rev. A* 85, 052324 (2012).
- [21] Tripathi, V. et al. Suppression of crosstalk in superconducting qubits using dynamical decoupling. *Phys. Rev. Appl.* 18, 024068 (2022).
- [22] Ezzell, N., Pokharel, B., Tewala, L., Quiroz, G. & Lidar, D. A. Dynamical decoupling for superconducting qubits: A performance survey. *Phys. Rev. Appl.* 20, 064027 (2023).
- [23] Zanardi, P. Symmetrizing evolution. Phys. Lett. A 258, 77 (1999).
- [24] Viola, L., Knill, E., & Lloyd, S. Dynamical generation of noiseless quantum subsystems. *Phys. Rev. Lett.* 85, 3520 (2000).
- [25] Lidar, D. A. Towards fault tolerant adiabatic quantum computation. *Phys. Rev. Lett.* 100, 160506 (2008).
- [26] West, J. R., Lidar, D. A., Fong, B. H. & Gyure, M. F. High fidelity quantum gates via dynamical decoupling. *Phys. Rev. Lett.* 105, 230503 (2010).
- [27] Byrd, M. S. & Lidar, D. A. Comprehensive encoding and decoupling solution to problems of decoherence and design in solid-state quantum computing. *Phys. Rev. Lett.* 89, 047901 (2002).
- [28] Ng, H. K., Lidar, D. A. & Preskill, J. Combining dynamical decoupling with fault-tolerant quantum computation. *Phys. Rev.* A 84, 012305 (2011).
- [29] Zhao, P. Z., Wu, X. & Tong, D. M. Dynamical-decoupling-protected nonadiabatic holonomic quantum computation. *Phys. Rev. A* 103, 012205 (2021).
- [30] Xu, G. F. & Long, G. L. Protecting geometric gates by dynamical decoupling. *Phys. Rev. A* 90, 022323 (2014).
- [31] Wu, X. & Zhao, P. Z. Universal nonadiabatic geometric gates protected by dynamical decoupling. *Phys. Rev. A* 102, 032627 (2020).
- [32] Wu, C. F., Sun, C. F., Chen, J. L. & Yi, X. X. Decoherence-Protected implementation of quantum gates. *Phys. Rev. Appl.* 19, 034069 (2023).
- [33] Souza, A. M., Álvarez, G. A. & Suter, D. Experimental protection of quantum gates against decoherence and control errors.

- Phys. Rev. A 86, 050301(R) (2012).
- [34] Suter D. & Álvarez, G. A. Protecting quantum information against environmental noise. Rev. Mod. Phys. 88, 041001 (2016).
- [35] Zhang, J. F., Souza, A. M., Brandao, F. D. & Suter, D. Protected quantum computing: Interleaving gate operations with dynamical decoupling sequences. *Phys. Rev. Lett.* 112, 050502 (2014).
- [36] Hart, T. P. et al. High-fidelity preparation, gates, memory, and readout of a trapped-ion quantum bit *Phys. Rev. Lett.* 113, 220501 (2014).
- [37] Barends, R. et al. Superconducting quantum circuits at the surface code threshold for fault tolerance. *Nature* 508, 500 (2014).
- [38] Evered, S. J. et al. High-fidelity parallel entangling gates on a neutral-atom quantum computer. *Nature* **622**, 268 (2023).
- [39] Zhang, J. F., Suter, D. Experimental protection of two-qubit quantum gates against environmental noise by dynamical decoupling. *Phys. Rev. Lett.* 115, 110502 (2015).
- [40] van der Sar, T. et al. Decoherence-protected quantum gates for a hybrid solid-state spin register. *Nature* 484, 82 (2012).
- [41] Liu, G., Po, H. C., Du, J., Liu, R. B. & Pan, X. Y. Noise-resilient quantum evolution steered by dynamical decoupling. *Nat. Commun.* 4, 2254 (2013).
- [42] Khodjasteh, K. & Viola, L. Dynamically error-corrected gates for universal quantum computation. *Phys. Rev. Lett.* 102, 080501 (2009).
- [43] Khodjasteh, K. & Viola, L. Dynamical quantum error correction of unitary operations with bounded controls. *Phys. Rev. A* 80, 032314 (2009).
- [44] Khodjasteh, K., Lidar, D. A. & Viola, L. Arbitrarily accurate dynamical control in open quantum systems. *Phys. Rev. Lett.* 104, 090501 (2010).
- [45] Mousolou, V. A., Canali, C. M. & Sjöqvist, E. Universal non-adiabatic holonomic gates in quantum dots and single-molecule magnets. *New J. Phys.* 16, 013029 (2014).
- [46] Doherty, M. W. et al. The nitrogen-vacancy colour centre in diamond. *Phys. Rep.* 528, 1 (2013).
- [47] Javadi-Abhari, A. et al. Quantum computing with Qiskit. arXiv:2405.08810.
- [48] Zeng, J., Yang, C. H., Dzurak, A. S. & Barnes, E. Geometric formalism for constructing arbitrary single-qubit dynamically corrected gates. *Phys. Rev. A* 99, 052321 (2019).

- [49] Dong, W., Zhuang, F., Economou, S. E. & Barnes, E. Doubly geometric quantum control. *PRX Quantum* 2, 030333 (2021).
- [50] Yi, K. et al. Robust quantum gates against correlated noise in integrated quantum chips *Phys. Rev. Lett.* 132, 250604 (2023).
- [51] Montangero, S., Calarco, T. & Fazio, R. Robust optimal quantum gates for Josephson charge qubits. *Phys. Rev. Lett.* 99, 170501 (2007).
- [52] Rebentrost, P., Serban, I., Schulte-Herbrüggen, T. & Wilhelm., F. K. Optimal control of a qubit coupled to a mon-Markovian environment. *Phys. Rev. Lett.* **102**, 090401 (2009).
- [53] Tsai, D. B., Chen, P. W. & Goan, H. S. Optimal control of the silicon-based donor-electron-spin quantum computing. *Phys. Rev. A* 79, 060306(R) (2009).
- [54] Motzoi, F., Gambetta, M., Merkel, S. T. & Wilhelm, F. K. Optimal control methods for rapidly time-varying Hamiltonians. *Phys. Rev. A* 84, 022307 (2011).
- [55] Huang, C. H. & Goan, H. S. Robust quantum gates for stochastic time-varying noise. *Phys. Rev. A* **95**, 062325 (2017).
- [56] Larrouy, A. et al. Fast navigation in a large Hilbert space using quantum optimal control. *Phys. Rev. X* 10, 021058 (2020).
- [57] Calzavara, M. et al. Optimizing optical potentials with physicsinspired learning Algorithms. *Phys. Rev. Appl.* 19, 044090 (2023).
- [58] Halaski, A., Krauss, M. G., Basilewitsch, D. & Koch., C. P. Quantum optimal control of squeezing in cavity optomechanics. *Phys. Rev. A* 110, 013512 (2024).
- [59] Li, B., Calarco, T. & Motzoi, F. Experimental error suppression in Cross-Resonance gates via multi-derivative pulse shaping. *npj Quantum Information* 10, 66 (2024).
- [60] Zahedinejad, E., Ghosh, J. & Sanders, B. C. Designing high-fidelity single-shot three-qubit gates: A machine-learning approach. *Phys. Rev. Appl.* 6, 054005 (2016).
- [61] Niu, M. Y., Boixo, S., Smelyanskiy, V. N. & Neven, H. Universal quantum control through deep reinforcement learning. *npj Quantum Inf.* 5, 33 (2019).
- [62] Fillingham, Z., Nevisi, H. & Dora, S. Optimisation of pulse waveforms for qubit gates using deep learning. arXiv:2408.02376.
- [63] Wang, Z. Y. & Liu, R. B. No-go theorems and optimization of dynamical decoupling against noise with soft cutoff. *Phys. Rev.* A 87, 042319 (2013).
- [64] Pan, Y., Xi, Z. R. & Gong, J. Optimized dynamical decoupling sequences in protecting two-qubit states. J. Phys. B 44, 175501 (2011).